

TLS-Based Quantification of Mangrove Drag for Numerical Wave Modeling

Putu Harry Gunawan^{1,*}, Irma Palupi¹, Ketut Tomy Suhari², Yusuf Muhammad²,
I Nyoman Giri Putra³, Gede Surya Indrawan³, I Putu Yogi Darmendra³, Gde Palguna Reganata⁴

¹CoE HUMIC, School of Computing, Telkom University, Bandung, 40257, West Java, Indonesia

²Department of Geodesy Engineering, Faculty of Civil Engineering and Planning, Institut Teknologi Nasional Malang, Malang 65145, Indonesia

³Marine Science Program, Faculty of Marine and Fisheries, Udayana University, Jimbaran, 80361, Bali, Indonesia

⁴Department of Informatics, Bali International University, Denpasar, 80234, Bali, Indonesia

Received September 18, 2025; Revised December 26, 2025; Accepted January 12, 2026

Cite This Paper in the Following Citation Styles

(a): [1] Putu Harry Gunawan, Irma Palupi, Ketut Tomy Suhari, Yusuf Muhammad, I Nyoman Giri Putra, Gede Surya Indrawan, I Putu Yogi Darmendra, Gde Palguna Reganata, "TLS-Based Quantification of Mangrove Drag for Numerical Wave Modeling," *Civil Engineering and Architecture*, Vol.14, No.2, pp. 858-868, 2026. DOI: 10.13189/cea.2026.140214.

(b): Putu Harry Gunawan, Irma Palupi, Ketut Tomy Suhari, Yusuf Muhammad, I Nyoman Giri Putra, Gede Surya Indrawan, I Putu Yogi Darmendra, Gde Palguna Reganata (2026). *TLS-Based Quantification of Mangrove Drag for Numerical Wave Modeling*. *Civil Engineering and Architecture*, 14(2), 858-868. DOI: 10.13189/cea.2026.140214.

Copyright ©2026 by authors, all rights reserved. Authors agree that this article remains permanently open access under the terms of the Creative Commons Attribution License 4.0 International License

Abstract Accurate characterization of the structure of mangrove forests is crucial to understanding their role in coastal protection and ecosystem dynamics. This study evaluates the use of Terrestrial Laser Scanning (TLS) for high-resolution, nondestructive measurement of mangrove morphological parameters in the dense forest environment of the TAHURA Nguurah Rai (Benoa), Bali. A Trimble X9 scanner was used to generate 3D point clouds in a 200×200 m² area, capturing detailed structural features of *Rhizophora mucronata*, including stems, canopies, and prop roots. Comparative analysis between 60 measurements of the diameter of the TLS derived from manual stems showed strong agreement, with a coefficient of determination of $R^2 = 0.8523$, a root mean square error (RMSE) of 0.00145, and a nonsignificant paired t-test result ($p = 0.815$), confirming the precision and statistical equivalence of the measurements based on TLS. The structural parameters of 30 trees in a representative 10×10 m² subdomain were extracted to calculate the volume of vegetation and the frontal area. These inputs were used to estimate drag coefficients (C_D), which yielded a mean value of 0.759, which closely aligns with previously reported reference values ($C_D = 0.725$). The results highlight the reliability of TLS for quantifying vegetation-induced hydraulic resistance and support its integration into hydrodynamic models for the assessment of wave attenuation. TLS-based structural mapping offers significant advantages for scalable and reproducible ecological modeling in mangrove-protected coastal zones.

Keywords Terrestrial Laser Scanning (TLS), Mangrove

Forests, Vegetation-Induced Drag Coefficient, Wave Attenuation Modeling

1 Introduction

Mangrove forests are widely recognized for their essential role in coastal protection, especially in dissipating wave energy and mitigating erosion during extreme weather events [1, 2]. Their complex root systems and above-ground biomass provide natural barriers that reduce wave force and protect vulnerable shorelines [3]. Quantifying the structural attributes of mangroves, such as trunk diameter, stem density, and root distribution, is vital for integrating vegetation effects into hydrodynamic and wave propagation models [4, 5].

However, accurate, scalable, and site-specific data on mangrove morphology remain difficult to obtain. Traditional field-based methods for collecting structural information are labor-intensive, time-consuming, and often constrained by accessibility in tidal, muddy, or densely vegetated zones [6, 7]. Moreover, these manual approaches are typically limited in spatial resolution and suffer from observer bias, restricting their effectiveness in representing the spatial heterogeneity of mangrove forests. This presents a significant methodological gap in the modeling of vegetation-induced drag and wave attenuation, particularly when attempting to scale models to regional or landscape levels.

Recent advances in Terrestrial Laser Scanning (TLS) technology offer a promising solution to this challenge. TLS can capture high-resolution three-dimensional (3D) point clouds of vegetation structures, allowing researchers to extract detailed morphological parameters non-destructively and with high precision [8, 9]. In forestry and ecological studies, TLS has shown great potential in estimating the structure of vegetation for applications ranging from biomass assessment to modeling fluid-structure interaction [10]. Despite this, its application in coastal mangrove ecosystems, especially for hydrodynamic modeling purposes—has not been fully explored or validated. There is a clear research gap in using TLS metrics derived to compute hydrodynamic drag coefficients, which are critical inputs in wave-vegetation interaction models.

This study addresses this gap by applying TLS in the Bena Mangrove Forest (TAHURA Ngurah Rai) in Bali, Indonesia, to quantify key structural parameters of mangroves relevant to wave resistance modeling. The TLS-derived data—specifically frontal area, stem diameter, and porosity—are used to estimate drag coefficients, which are then evaluated against values derived from traditional direct field measurements. By doing so, this research evaluates the validity and potential advantages of TLS as a tool to improve the realism and efficiency of coastal hydrodynamic simulations.

Ultimately, this study contributes to advancing the integration of remote sensing and ecological modeling, providing a practical framework for incorporating high-resolution vegetation structure data into numerical models for wave attenuation. The findings are expected to support improved design and validation of nature-based coastal defense strategies, particularly in tropical and developing regions vulnerable to sea-level rise and storm impacts.

The remainder of this paper is organized into four sections. Section 2 presents the research methodology, including the 3D Terrestrial Laser Scanning (TLS) workflow. Section 3 discusses the results, highlighting the morphological characteristics extracted from the TLS data. Finally, Section 4 concludes the study and outlines potential directions for future research.

2 Materials and Methods

2.1 Study Area

In this research, the characteristic of mangroves is important to calculate the drag coefficient. Each species of mangrove tree has different characteristics, such as the length of the roots, stem, and leaf. In order to obtain the characteristic of mangroves tree, this research uses a 3D laser scanner. The data from the 3D laser scanner were then analyzed to get the details of the measurement. The details of our research methodology can be found in Figure 1.

Following the research methodology in Figure 1, the research questions for this research are:

1. How can Terrestrial Laser Scanning (TLS) be utilized to effectively visualize and extract structural characteristics of mangrove trees in dense forest environments?

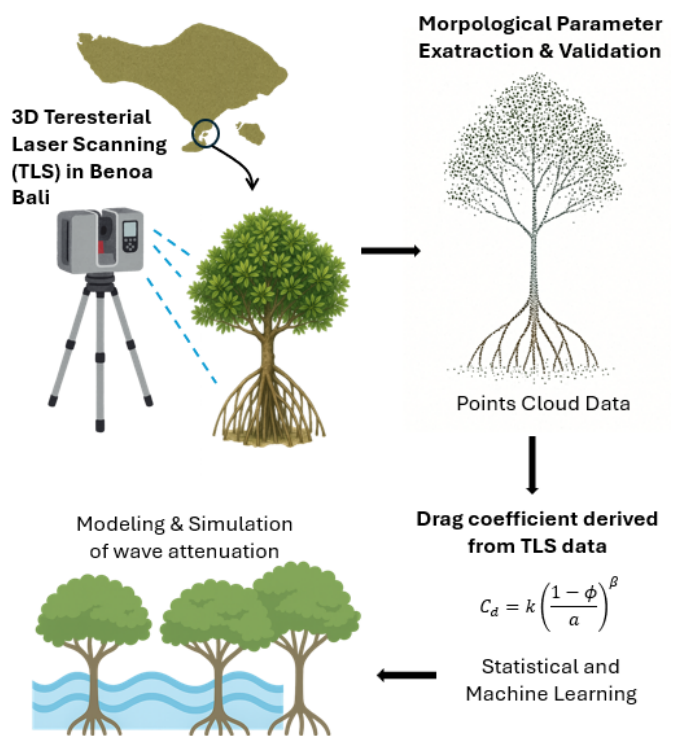


Figure 1. Overview of research methodology

2. To what extent does the accuracy of TLS-derived measurements compare with traditional manual measurements in quantifying mangrove stem characteristics within densely vegetated areas?
3. How can TLS-based quantification of mangrove morphological parameters be used to derive drag coefficients applicable to wave attenuation modeling in the Bena TAHURA mangrove forest, Bali?

The mangrove data used in this study were collected from a selected site within the Bena Mangrove Forest, officially designated as TAHURA (Taman Hutan Raya) Ngurah Rai, Bali. The study area is geographically located at the coordinates $8^\circ 43' 30.9''\text{S}$ and $115^\circ 12' 00.9''\text{E}$. This specific site was chosen for its strategic accessibility and suitability for the installation and operation of a Terrestrial Laser Scanner (TLS) system.

TAHURA represents a significant mangrove conservation zone extending along the southern coast of Bali, covering areas from Sanur to Bena, Ngurah Rai and Jimbaran. It plays a vital ecological role by preserving the biodiversity of mangrove species and serving as a natural barrier against coastal erosion and saline intrusion. The location of the survey site is illustrated in Figure 2.



Figure 2. Survey site in the Mangrove Forest of TAHURA Bali (top) and visual depiction of the dense mangrove trees in the study area (bottom).

The dominant mangrove species identified at the survey site belongs to the genus *Rhizophora*, specifically *Rhizophora mucronata*, consistent with the findings of previous studies [11, 12]. A defining characteristic of *R. mucronata* is the presence of prominent stilt roots, which extend from the trunk and lower branches, providing mechanical stability on the soft, waterlogged substrate typical of intertidal zones.

The species has dark green, glossy leaves with distinctive black dots on the paler underside and a pointed apex that is often broken. The reproductive strategy includes vivipary, in which propagules (seedlings) germinate while still attached to the parent tree and eventually fall to establish new individuals in the mud. These physiological and morphological adaptations enable the species to thrive in saline and dynamic coastal environments, significantly contributing to coastal protection, carbon sequestration, and ecosystem productivity.

Field observations indicated that the average tree height of *R. mucronata* in the study area is approximately 20 m. The dense canopy and complex root systems presented an ideal scenario for evaluating TLS-based structural characterization methods.

2.2 TLS Data Acquisition and Instrumentation

3D Terrestrial Laser Scanning (TLS) is a ground-based remote sensing technology that enables high-resolution, three-dimensional mapping of physical environments. TLS systems employ laser pulses to measure the distances between the scanner and objects within its field of view, resulting in dense point clouds that represent the geometry of the scanned surfaces [13, 14]. This technique has become a cornerstone in

geospatial surveying, structural monitoring, and documentation in various industries.

TLS systems typically operate using one of two primary methods [15, 16, 17]:

- **Time-of-Flight (ToF):** Measures the time a laser pulse takes to travel to an object and return. This method is effective for long-range scanning.
- **Phase-Shift Scanning:** Measures the phase difference between emitted and received light waves to calculate distances with high precision over short to medium ranges.

Modern TLS instruments rotate horizontally and vertically to systematically scan the environment, producing millions of data points in a matter of minutes. Each point is recorded with its x , y , z coordinates and often with color or intensity values.

Several manufacturers produce high-precision terrestrial laser scanners suited for various applications in engineering, construction, and geospatial sciences. Leading vendors and their commonly used systems include:

- **Leica Geosystems:** Offers a range of TLS devices such as the Leica C10 and BLK360 [18]. These systems are widely used in architecture, surveying, and heritage documentation due to their reliability and integration with BIM workflows.
- **FARO Technologies:** The FARO Focus series (e.g. Focus Premium and Focus Premium Max) provides highly accurate and portable TLS solutions with scanning ranges up to 350–400 meters. They are suitable for industrial inspections, forensics, and civil engineering projects [19].
- **RIEGL:** Known for the VZ-series terrestrial scanners, RIEGL devices are often used in mining, topography, and forestry due to their long-range and high-speed scanning capabilities [20].
- **Trimble:** Trimble X9 and X7 scanners are designed for construction, structural monitoring, and geospatial surveys, offering robust field performance and efficient data workflows [21, 22, 23].
- **Topcon:** GLS series scanners are used in construction, infrastructure inspection, and facility management, with a focus on a user-friendly interface and accurate deliverables [24].

Accurate structural characterization of mangrove vegetation requires a noninvasive high-resolution sensing technique with reliable geometric precision. In this study, a terrestrial laser scanner (TLS) was used to collect detailed three-dimensional point clouds across the mangrove plot. The TLS hardware, scanning configuration, and accuracy considerations are summarized below.

Hardware and System Configuration. The field survey used a terrestrial laser scanner equipped with a full 360° horizontal and 300° vertical field of view, enabling comprehensive coverage of the dense mangrove canopy and root structures. The instrument operates using a time-of-flight laser ranger

method, acquiring measurements with millimeter-level accuracy at medium ranges, consistent with the performance of modern TLS systems [13, 14]. The Manufacturer-specified accuracy was incorporated into the scanning plan to minimize positional error and occlusion.

Scanning Setup and Data Capture. To ensure complete coverage of the vegetation structure, scans were conducted from multiple vantage points surrounding the plot. Each scan was performed using the following configuration:

1. Alignment of the TLS coordinate system with ground control points (GCPs) established during manual measurements.
2. Performing 360° scans with high-density point acquisition to reduce shadowing caused by dense roots and canopy.
3. Adjusting scanning resolution according to the distance to the target, with finer resolution applied to roots and stems within 10 to 20 meters of the scanner.
4. Storing raw point-cloud data in LAS/E57 format for subsequent processing and registration.

Accuracy and Quality Control. To ensure geometric reliability, each scan was visually inspected for noise, multipath artifacts, and occlusions. Registration accuracy was assessed using target-to-target alignment, achieving sub-centimeter residuals after merging the scans. These measures comply with best practices in TLS-based vegetation surveys [15, 17].

All instruments used in the TLS and manual survey, including the Electronic Total Station (ETS), TLS unit, and premark reference markers, are shown in Figure 3.

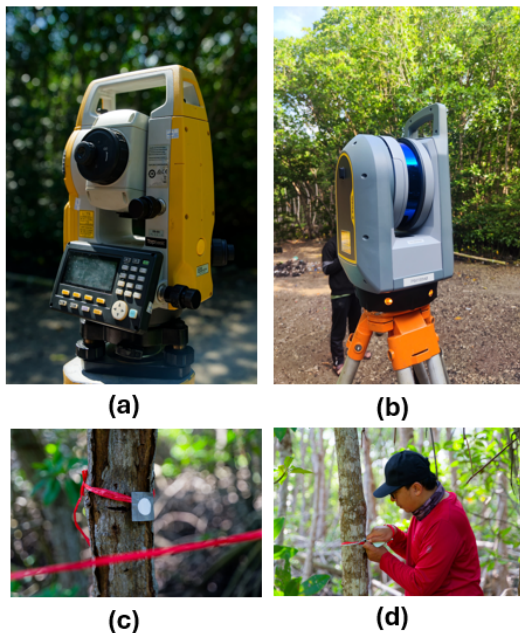


Figure 3. Field instrumentation used in the survey: (a) Electronic Total Station (ETS), (b) terrestrial laser scanner (TLS), (c) premark reference markers for ETS–TLS georeferencing, and (d) manual diameter measurement.

2.3 Manual Data Collection and Validation

Manual measurements were conducted to validate the geometric parameters derived from TLS and to establish reference coordinates for scan registration. The manual protocol followed standard forest and surveying procedures to ensure consistency and precision in all measurements.

Ground Control and Positioning. The reference coordinates were first established using a geodetic-grade GPS receiver. These points served as ground control points (GCPs) for aligning the TLS dataset. Premark targets were placed on selected tree trunks to enable direct sighting by the Electronic Total Station (ETS).

Electronic Total Station (ETS) Survey. The ETS was used to determine the precise positions of the mangrove trees and the premark targets. The protocol included:

1. Setting up the ETS on a stable benchmark with known GPS coordinates.
2. Seeing each premark target to record its x, y, z coordinates.
3. Measurement of angular directions and distances to each tree location.
4. Recording of all coordinates to construct an accurate 2D–3D spatial reference network.

Manual Validation Measurements. The diameter of the stem was measured using a measuring tape at a consistent height (1.3 m above the ground, following the DBH standard). Each measurement was repeated twice to reduce human error, and the averaged values were used for validation. These manual observations serve as ground truth for assessing TLS accuracy, particularly in diameter estimation and tree positioning.

Field activities demonstrating TLS and manual data collection are illustrated in Figure 3.

2.4 Parameter Extraction

According to Teh et al. [25], the resistance induced by mangroves can be formulated based on the classical Morison equation, which captures the hydrodynamic forces exerted on rigid cylindrical elements representing the components of the tree. The morphological structure of the mangrove trees—canopy, stem, and root—is modeled by their respective diameters (D_l, D_s, D_r) and heights (H_l, H_s, H_r). These components are illustrated in Figure 4.

For a rigid cylinder of diameter D , the inline Morison equation for force per unit length is expressed as:

$$F_{\text{Morison}} = \frac{1}{2} \rho C_D A_0 |U|U + \rho C_M \frac{\pi A_0^2}{4} \frac{dU}{dt}, \quad (1)$$

where ρ is the density of the fluid, C_D is the drag coefficient, C_M is the added mass coefficient, A_0 is the projected area of trees on the surface of the water, and $U(t)$ is the local flow velocity relative to the vegetation structure.

The drag coefficient C_D is parameterized as a function of mangrove morphology and spatial density [25] using:

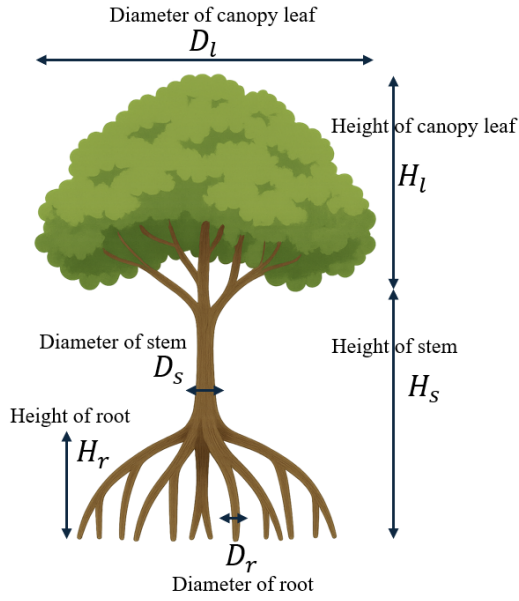


Figure 4. Schematic of mangrove tree components used in friction modeling.

$$C_D = \frac{840 \frac{V_{obs}}{V} + 66}{100}, \quad \left(\frac{1}{100} \leq \frac{V_{obs}}{V} \leq \frac{7}{100} \right), \quad (2)$$

where V_{obs} is the volume of vegetative solids in water and V is the control volume.

The value of A_0 and V_{obs} can be determined by measuring mangrove characteristics using the TLS. Here are the calculations of A_0 and V_{obs} based on the three characteristics of mangroves, as shown in Figure 4:

$$A_0 = A_{root} + A_{stem} + A_{leaf}, \quad (3)$$

where

$$A_{root} = H_r \left(D_r \frac{N_r N_s}{100} \right), \quad A_{stem} = H_s \left(D_s \frac{N_s}{100} \right),$$

$$A_{leaf} = H_l \left(P_l D_l \frac{N_s}{100} \right),$$

and

$$V_{obs} = V_{root} + V_{stem} + V_{leaf}, \quad (4)$$

where

$$V_{root} = H_r \left(\frac{\pi D_r^2 N_r N_s}{4} \right), \quad V_{stem} = H_s \left(\frac{\pi D_s^2 N_s}{4} \right),$$

$$V_{leaf} = H_l \left(\frac{\pi P_l D_l^2 N_s}{4} \right).$$

Here, the number of stems in the area $10 \text{ (m}^2\text{)}$ and the number of roots per tree are denoted by N_s and N_r , respectively. Moreover, P_l denotes the porosity of the leaf.

2.5 Numerical Wave Modeling in Mangrove-Enclosed Areas

Mangrove stands act as emergent or submerged porous structures that impose both form drag and inertial resistance on depth-averaged flows. Within the framework of shallow-water modeling, the hydrodynamic influence of mangrove vegetation is typically introduced through additional momentum source terms. These vegetation-induced forces are often described using a *Morison-type* formulation, consisting of a nonlinear (quadratic) drag term and a linear inertial term.

Let $h(x, t)$ denote the depth of the water and $u(x, t)$ the velocity averaged by depth in a one-dimensional domain. Conservative shallow-water equations (SWEs), without vegetation-induced friction, are written as follows [26, 27, 28]:

$$\frac{\partial h}{\partial t} + \frac{\partial}{\partial x}(hu) = 0, \quad (5)$$

$$\frac{\partial(hu)}{\partial t} + \frac{\partial}{\partial x}(hu^2 + \frac{1}{2}gh^2) = -gh \frac{\partial z_b}{\partial x}, \quad (6)$$

where g is the gravitational acceleration and $z_b(x)$ is the elevation of the bed. In this basic formulation, frictional resistance due to vegetation is not yet considered. To realistically simulate mangrove–wave interactions, the frictional effects of vegetation must be introduced.

Incorporating vegetation-induced resistance from (1), the momentum conservation equation (6) is modified as:

$$\frac{\partial(hu)}{\partial t} + \frac{\partial}{\partial x}(hu^2 + \frac{1}{2}gh^2) = -gh \frac{\partial z_b}{\partial x} - F_{Morison}. \quad (7)$$

This modified shallow-water system, enhanced with vegetation drag, provides a more realistic framework to simulate wave dissipation, current attenuation, and energy loss due to mangrove stands.

Numerical Considerations Several numerical methods have been used to solve the above system, including finite-volume approaches with collocated grids [27, 28] or staggered grids [26, 29]. These methods ensure an accurate representation of the hydrodynamic variables and momentum fluxes, especially in complex and vegetated bathymetric environments.

3 Results and Discussion

3.1 Laser Scanner Results

In this study, a total area of $200 \times 200 \text{ m}^2$ within the mangrove forest at the TAHURA Benoa Bali site was scanned using a terrestrial laser scanner (TLS) with the Trimble X9. The use of TLS allows for the generation of a high-resolution 3D point cloud, capturing the complex geometry of the mangrove forest structure in fine detail.

The TLS scan revealed a detailed three-dimensional vegetation architecture, capturing canopy topography, as well as the internal arrangement of branches and root structures—features

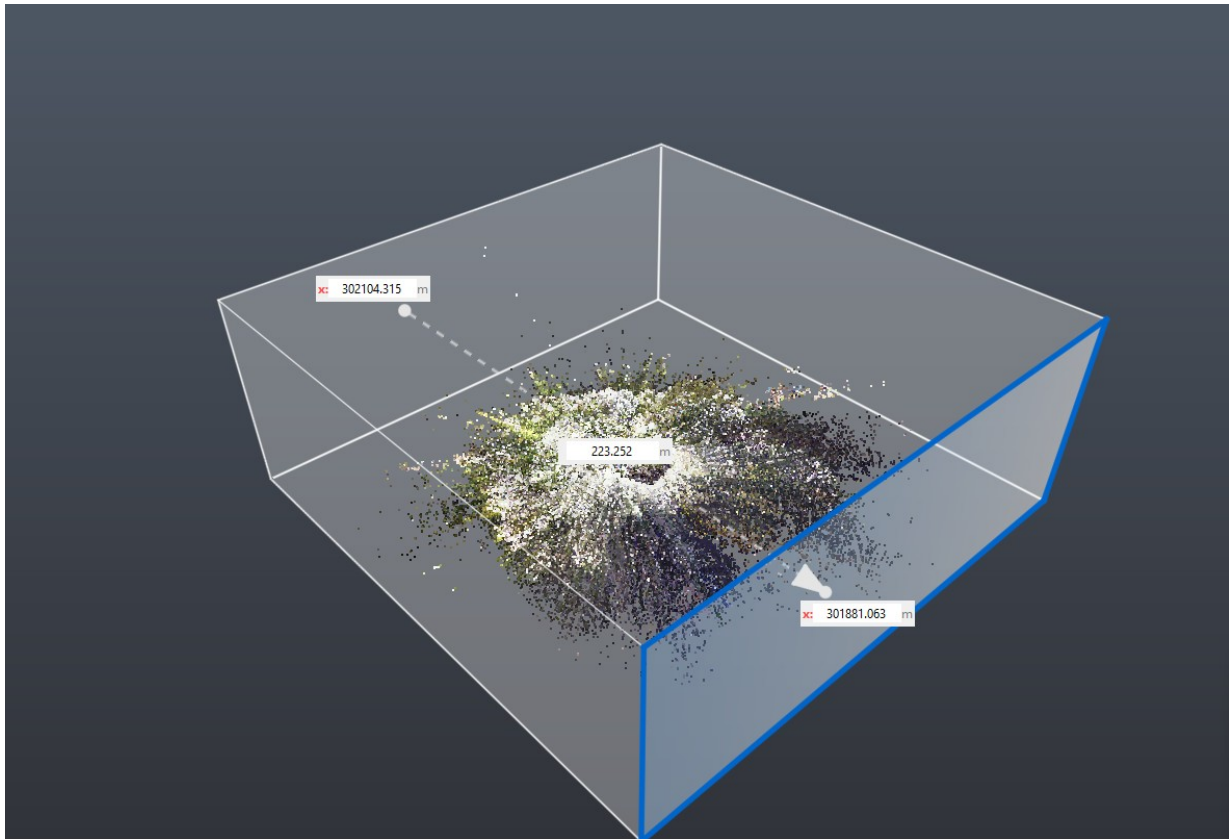


Figure 5. The results of point cloud scanning using 3D TLS over a $200 \times 200 \text{ m}^2$ domain in the TAHURA mangrove forest.

essential to estimate vegetation density, porosity, and frontal area used in hydrodynamic drag modeling (Figure 5). The visualization provides a clear frontal perspective that highlights the volume and depth distribution of the scanned mangrove structure, allowing accurate structural interpretation.

These 3D point cloud datasets are crucial for the next stage of the analysis, which involves extracting the morphological characteristics of mangrove trees, such as canopy height, trunk diameter, and distribution density, by segmenting and classifying the TLS data. These features will serve as a quantitative input for modeling the drag force exerted by mangrove vegetation on wave and current flow, as discussed in the hydrodynamic modeling section.

In addition, the point cloud facilitates comparison with manual measurements to validate the accuracy and resolution of the morphological parameters derived from TLS. The comprehensive spatial coverage and vertical resolution of TLS offer significant advantages in dense mangrove stands, where traditional field measurement approaches may be limited by accessibility and visibility.

3.2 Stem Diameter Measurement: Manual vs TLS

This section presents a comparison between *manual* and *TLS-derived* stem diameter measurements for mangrove trees in the Benoa Mangrove Forest (TAHURA Ngurah Rai). The analysis combines visual inspection and statistical testing to evaluate the accuracy and equivalence of the TLS measurements. A dataset consisting of 60 pairs of stem diameters was

collected from the Benoa Mangrove Forest (TAHURA Ngurah Rai) (see Figure 6).



Figure 6. The 60 random samples of mangrove trees for manual observation.

A scatter plot was generated to visualize the relationship between manual and TLS measurements (Figure 7). Each point represents one observation of the diameter of the stem, with manual measurement values on the x-axis and TLS values on the y-axis.

The data points show a strong alignment along the red dashed 1:1 reference line, indicating a close agreement between manual and TLS-based stem diameter measurements (Figure 7). The close clustering around this diagonal line indicates a high degree of linearity and suggests that TLS is capable of capturing stem diameter values with accuracy comparable to traditional manual methods throughout the range of measurements. Furthermore, there is no evident pattern of systematic bias, neither consistent overestimation nor underestimation, by

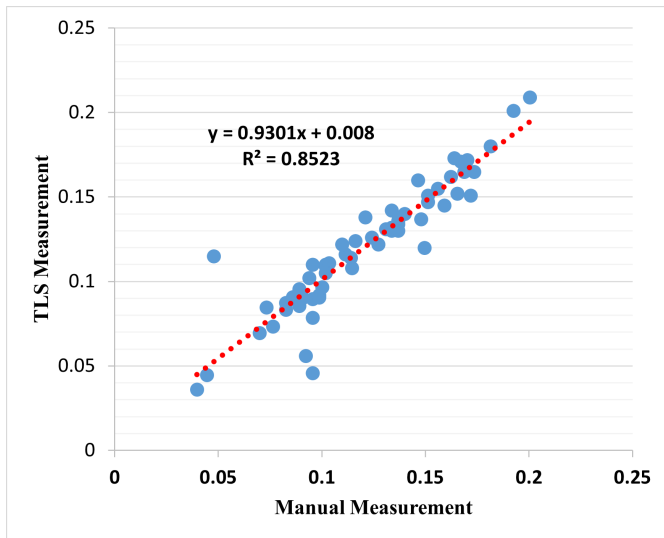


Figure 7. Accuracy comparison of stem diameter measurements using manual observations and TLS data.

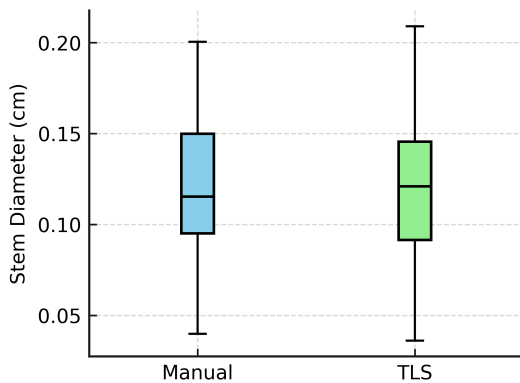


Figure 8. Boxplot comparison of manual and TLS measurements of stem diameter. Both distributions appear statistically similar.

the TLS measurements. Quantitatively, the coefficient of determination ($R^2 = 0.8523$) and the low root mean square error (RMSE = 0.00145) both support the conclusion that TLS provides reliable and precise diameter estimates in dense mangrove environments.

To further explore the distribution of the measurements, a boxplot comparison was conducted (Figure 8). Both manual and TLS datasets show nearly identical medians, interquartile ranges, and overall spread, with no significant outliers in either group.

This visual consistency demonstrates that not only are the individual measurements comparable (as shown in the scatter plot), but also the overall distributions of both datasets are statistically similar. These results support the reliability of the TLS in representing the structural characteristics of mangrove stems.

To statistically validate the similarity between manual and TLS measurements, a paired t-test was performed. The test resulted in a test statistic of $t = 0.235$ and a p -value of 0.815, which is well above the conventional significance threshold ($\alpha = 0.05$).

$$t = 0.235 \quad ; \quad p = 0.815$$

Since the value of p exceeds the significance level, we do not reject the null hypothesis. This result confirms that there are no statistically significant differences between the two sets of measurements. Thus, TLS can be considered a valid and statistically equivalent method to manual measurement to capture stem diameters in this context.

3.3 Quantifying Mangrove Structure from TLS Data

To determine the drag coefficient in Equation (2) specific to the dominant mangrove species at the survey site, a detailed quantification of the forest structure of the 3D TLS point clouds is essential. Within a representative $10 \times 10, \text{m}^2$ sub-domain, a total of 30 individual mangrove trees were identified and analyzed, capturing the dense arrangement of tall trees with an average height of approximately 20,m—characteristic of the stands of *Rhizophora mucronata* observed in the field (Figure 9, Right).

In this study, visualization and processing of 3D TLS point cloud data were performed using Autodesk® ReCap™ Pro—a specialized software tool designed for high-resolution laser scanning analysis. ReCap Pro offers a comprehensive suite of features for managing and interpreting point-cloud data, including filtering noise, registering multiple scans, and applying georeferencing to align spatial data with global coordinate systems. It also allows for segmentation and cropping of specific regions of interest, facilitating focused analysis on individual tree specimens.

Advanced visualization modes in ReCap Pro allow researchers to examine point clouds based on color attributes (e.g., RGB), elevation values, or reflectance intensity. Additionally, photogrammetric integration enables georeferenced imagery to be overlaid on the 3D data, enhancing both qualitative and quantitative interpretation. The measurement tools within the software allow for precise extraction of tree morphometrics, including height, diameter of the stem, dimensions of the canopy, and characteristics of the roots [30].

A close-up visualization of an individual mangrove tree extracted from the TLS data reveals detailed structural features, allowing precise measurement of root, stem and leaf heights, as well as their respective diameters, using the built-in tools of ReCap Pro (Figure 9, Left). This level of structural quantification provides the necessary inputs to derive vegetation-induced hydraulic resistance parameters, including the drag coefficient C_D , which is fundamental to modeling wave–vegetation interactions.

Quantification of mangrove structural characteristics from the TLS point cloud is necessary to estimate vegetation-induced hydrodynamic resistance. In this study, a total of 30 mangrove tree samples were identified and extracted from a domain $10 \times 10 \text{m}^2$. The processed data includes detailed measurements of the canopy, stem, and root dimensions for each individual tree.

Table 1 presents the structural parameters at the sample level, where D_l , D_s , and D_r represent the diameters of the leaf



Figure 9. (Left) Example of a mangrove tree quantification from TLS point cloud. (Right) Overview of 30 individual mangrove trees identified within a $10 \times 10 \text{ m}^2$ domain.

Table 1. Structural parameters of individual mangrove trees

Sample	D_l	D_s	D_r	H_l	H_s	H_r
1	2.811	0.203	0.033	2.465	15.633	1.603
2	3.816	0.147	0.026	3.712	13.960	1.769
3	3.259	0.220	0.044	2.781	15.138	1.780
4	2.583	0.173	0.039	2.372	14.155	1.483
5	3.198	0.111	0.027	3.546	8.989	1.502
6	2.473	0.136	0.035	2.836	13.186	1.392
⋮	⋮	⋮	⋮	⋮	⋮	⋮
29	2.188	0.123	0.026	3.037	11.574	1.546
30	4.420	0.077	0.048	2.743	8.682	1.635

canopy, stem, and root, respectively, while H_l , H_s , and H_r denote their respective heights. The total volume observed in the domain is $V = 2000 \text{ m}^3$, corresponding to a maximum tree height of 20 meters and a tree count of 30 individuals. Based on field inspection, the average number of prop roots per tree was approximately 100.

To simplify the analysis, the structural parameters were summarized using three statistical measures: mean, minimum, and maximum, as shown in Table 2.

Using these summary statistics, the drag coefficient C_D was calculated based on Equation (2) with assumed root porosity $P_l = 0.03$. The resulting drag coefficient values for each scenario (mean, min, max) are shown in Table 3.

As observed in Table 3, the calculated drag coefficients for

Table 2. Summary statistics of structural parameters from mangrove tree samples

Parameter	Mean	Min	Max
D_l (Diameter of leaf canopy)	2.826	1.570	5.689
D_s (Diameter of stem)	0.129	0.083	0.220
D_r (Diameter of root)	0.033	0.020	0.047
H_l (Height of leaf canopy)	2.604	1.249	3.712
H_s (Height of stem)	11.608	6.660	15.633
H_r (Height of root)	1.748	0.654	3.195

Table 3. Summary of estimated drag coefficients (C_D) using $P_l = 0.03$

Parameter	Mean	Min	Max	Ref. [25]
V_{root} (m ³)	4.401	0.616	16.621	0.054
V_{stem} (m ³)	4.528	1.080	17.819	2.790
V_{leaf} (m ³)	14.694	2.175	84.877	12.717
V_{obs} (m ³)	23.623	3.872	119.317	15.569
V_{obs}/V	0.012	0.002	0.060	0.008
C_D	0.759	0.676	1.161	0.725

the observed samples are consistent with the reference values reported in the literature [25], demonstrating the viability of the TLS-based quantification method. The estimated C_D of the mean scenario is 0.759, which closely matches the reference value of 0.725. These findings confirm that the structural parameters derived from the TLS point clouds can effectively estimate vegetation-induced drag, which is essential to simulate wave attenuation in mangrove-protected coastal zones such as Benoa TAHURA, Bali.

4 Conclusions

This study demonstrates the effective application of terrestrial laser scanning (TLS) to capture and analyze the structural complexity of mangrove forests, particularly within the dense canopy of the TAHURA Ngurah Rai (Benoa) site in Bali. Through integrated visualization, quantitative comparison, and statistical validation, several important conclusions are drawn:

- TLS provides high-resolution, noninvasive 3D point cloud data that effectively capture detailed vegetative structures, such as stems, roots, and canopy layers, that are otherwise difficult to measure manually in dense mangrove stands.
- The comparison between manual and TLS-derived stem diameter measurements shows excellent agreement, confirmed by both graphical and statistical analyses. The coefficient of determination ($R^2 = 0.8523$) and a low root mean square error (RMSE = 0.00145) indicate high measurement accuracy, while a paired t-test ($p = 0.815$) validates that there is no statistically significant difference between the two methods. These findings confirm the reliability and precision of the structural assessment based on TLS in mangroves.
- The structural quantification of 30 individual *Rhizophora mucronata* trees within a $10 \times 10 \text{ m}^2$ plot yielded mean

values for the height of the stem ($H_s = 11.6 \text{ m}$), the diameter of the stem ($D_s = 0.129 \text{ m}$) and the dimensions of the roots ($H_r = 1.75 \text{ m}$, $D_r = 0.033 \text{ m}$). These morphological parameters are critical for estimating vegetation volume and frontal area, which directly inform the calculations of drag coefficients for hydrodynamic modeling.

- The derived drag coefficient ($C_D = 0.759$) closely matches the literature value ($C_D = 0.725$ [25]), validating the suitability of TLS-based morphology for hydrodynamic and coastal protection modeling. The observed variation ($0.676 \leq C_D \leq 1.161$) underscores the influence of structural heterogeneity on flow resistance and wave attenuation potential.
- In general, TLS-based quantification enables efficient, accurate, and reproducible characterization of mangrove vegetation, improving parameterization of the ecohydrodynamic model and supporting data-driven simulations of wave attenuation and coastal resilience.

Limitations

This study was conducted at a single site and focused solely on one mangrove species, *Rhizophora mucronata*. The drag coefficient estimation relied on several simplifying assumptions, including uniform leaf porosity and an average number of prop roots per tree, which may not fully represent interspecies or intra-species variability. Furthermore, the analysis did not directly couple the TLS-derived parameters with field-based hydrodynamic measurements, such as in situ wave or current data, limiting the direct validation of model results.

Future Work

Future research should extend TLS applications to multiple mangrove species (e.g., *Avicennia* and *Sonneratia*) with varying root and canopy architectures to better understand structural diversity and its hydrodynamic implications. Integrating TLS data with UAV photogrammetry could enhance spatial coverage and canopy mapping, while coupling with field-based wave and flow measurements would enable a more robust calibration of drag and attenuation models. Ultimately, combining multi-sensor datasets will strengthen the predictive accuracy of mangrove-based coastal protection and resilience assessments.

Acknowledgements

The authors express their sincere gratitude to the Ministry of Research, Technology and Higher Education of the Republic of Indonesia for supporting this research grant based on Decree Number 0419/C3/DT.05.00/2025 dated 22 May 2025 and Agreement / Contract Numbers 125/C3/DT.05.00/PL/2025 dated 28 May 2025; 7925/LL4/PG/2025 dated 4 June 2025 with LLDIKTI IV; and with a contract number with Telkom University: 097/LIT07/PPM-LIT/2025 dated 5 June 2025. The first and corresponding author is the Principal Investigator of

the grant. The authors also express special thanks to Alpuji, Nafi Udin, and Wandu Y. Kurniawan for their survey of data collection, and also to William A. Simanjutak for the documentation during data collection.

Author Contributorship

P.H.G. led the research, wrote the draft, defined the research scenario, and reviewed and revised the manuscript. I.P. analyzed the data in a mathematical model. K.T.S. and Y.M. conducted the field survey, collected and processed the data, and contributed to the visualization of results. I.N.G.P. analyzed the mangrove species and their habitat. G.S.I. designed the research location and controlled the tide data. I.P.Y.D. reviewed and proofread the manuscript. G.P.R. analyzed the results using statistical tools.

Data Availability

The authors declare that the data supporting the findings of this study are available in the article.

REFERENCES

- [1] X. Chen, Z. Yin, Z. Li, B. Wang, A. Tao, Z. Guo, F. Wang, Y. An, and K. O'Driscoll, "Overview on mangrove forest disaster prevention and mitigation functions," *Journal of Ocean University of China*, vol. 23, no. 1, pp. 46–56, 2024. DOI: 10.1007/s11802-024-5672-3
- [2] X. Xu, D. Fu, F. Su, V. Lyne, H. Yu, J. Tang, X. Hong, and J. Wang, "Global distribution and decline of mangrove coastal protection extends far beyond area loss," *Nature Communications*, vol. 15, no. 1, p. 10267, 2024. DOI: 10.1038/s41467-024-54349-0
- [3] A. Gijón Mancheño, V. Vuik, B. van Wesenbeeck, S. Jonkman, R. van Hespén, J. Moll, S. Kazi, I. Urrutia, and M. van Ledden, "Integrating mangrove growth and failure in coastal flood protection designs," *Scientific Reports*, vol. 14, no. 1, p. 7951, 2024. DOI: 10.1038/s41598-024-58705-4
- [4] J. W. Hill, V. Bennion, and C. E. Lovelock, "Mangrove tree strength estimated with field experiments," *Ecological Engineering*, vol. 203, p. 107259, 2024. DOI: 10.1016/j.ecoleng.2024.107259
- [5] A. J. Twomey and C. E. Lovelock, "Variation in mangrove geometric traits among genera and climate zones," *Estuaries and Coasts*, vol. 48, no. 2, p. 55, 2025. DOI: 10.1007/s12237-025-01487-3
- [6] S. Li, Z. Zhu, W. Deng, Q. Zhu, Z. Xu, B. Peng, F. Guo, Y. Zhang, and Z. Yang, "Estimation of above-ground biomass of different vegetation types in mangrove forests based on uav remote sensing," *Sustainable Horizons*, vol. 11, p. 100100, 2024. DOI: 10.1016/j.horiz.2024.100100
- [7] H. Niwa, H. Ise, and M. Kamada, "Suitable lidar platform for measuring the 3d structure of mangrove forests," *Remote Sensing*, vol. 15, no. 4, p. 1033, 2023. DOI: 10.3390/rs15041033
- [8] T. Dunlop, A. G. Mancheño, W. Glamore, S. Felder, and B. K. van Wesenbeeck, "Quantifying mangrove forest attributes using terrestrial laser scanning," *Estuaries and Coasts*, vol. 48, no. 4, p. 108, 2025. DOI: 10.1007/s12237-025-01533-0
- [9] M. Åkerblom and P. Kaitaniemi, "Terrestrial laser scanning: a new standard of forest measuring and modelling?" *Annals of Botany*, vol. 128, no. 6, pp. 653–662, 2021. DOI: 10.1093/aob/mcab111
- [10] M. Demol, H. Verbeeck, B. Gielen, J. Armston, A. Burt, M. Disney, L. Duncanson, J. Hackenberg, D. Kükenbrink, A. Lau *et al.*, "Estimating forest above-ground biomass with terrestrial laser scanning: Current status and future directions," *Methods in Ecology and Evolution*, vol. 13, no. 8, pp. 1628–1639, 2022. DOI: 10.1111/2041-210X.13906
- [11] N. M. Ernawati, I. A. Astarini, I. W. Suarna, A. As-Syakur, I. Y. Perwira, A. P. W. K. Dewi, I. P. Sugiana *et al.*, "Comparison of soil carbon-nitrogen ratio at two different mangrove ecosystem in bali, indonesia," *Ecological Engineering & Environmental Technology*, vol. 25, no. 7, pp. 343–354, 2024. DOI: 10.12912/27197050/188738
- [12] I. G. N. P. Dharmayasa, I. P. Sugiana, and P. Anantanasakul, "Mangrove species distribution across soil texture gradients in benoa bay and nusa lembongan, bali province, indonesia," *Biodiversitas Journal of Biological Diversity*, vol. 26, no. 6, 2025. DOI: 10.13057/biodiv/d260633
- [13] T. C. Matta, L. S. Pereira, Y. C. Belmonte, F. de Oliveira Chaves, and M. L. G. Soares, "Evaluating terrestrial laser scanning for structural characterization of mangrove forests in southeastern brazil," *Forest Ecology and Management*, vol. 583, p. 122567, 2025. DOI: 10.1016/j.foreco.2025.122567
- [14] A. Rouzbeh Kargar, R. A. MacKenzie, A. Fafard, K. W. Krauss, and J. van Aardt, "Surface elevation change evaluation in mangrove forests using a low-cost, rapid-scan terrestrial laser scanner," *Limnology and Oceanography: Methods*, vol. 19, no. 1, pp. 8–20, 2021. DOI: 10.1002/lom3.10401
- [15] A. Sun, L. Wang, W. Qian, J. Wang, S. Xu, and B. Wang, "A review of error analysis and calibration techniques for spherical coordinate 3d laser scanners: Focus on non-instrumental and non-geometric factors," *Measurement and Control*, p. 00202940241312667, 2025. DOI: 10.1177/00202940241312667

- [16] C. Wu, Y. Yuan, Y. Tang, and B. Tian, "Application of terrestrial laser scanning (tls) in the architecture, engineering and construction (aec) industry," *Sensors*, vol. 22, no. 1, p. 265, 2021. DOI: 10.3390/s22010265
- [17] A. Azam, A. H. Alshehri, M. Alharthai, M. M. El-Banna, A. M. Yosri, and A. A. Beshr, "Applications of terrestrial laser scanner in detecting pavement surface defects," *Processes*, vol. 11, no. 5, p. 1370, 2023. DOI: 10.3390/pr11051370
- [18] L. Kovanič, P. Blišťan, B. Topitzer, P. Pet'ovský, and R. Boczek, "Tls and low-cost uav photogrammetry as an effective combination of spatial data collection methods for creating detailed 3d surface models (dem)," *GIS Odyssey Journal*, vol. 3, no. 1, 2023. DOI: 10.57599/gisoj.2023.3.1.163
- [19] J. Balado, E. Frías, S. M. González-Collazo, and L. Díaz-Vilariño, "New trends in laser scanning for cultural heritage," in *New Technologies in Building and Construction: Towards Sustainable Development*, Springer, pp. 167–186, 2022. DOI: 10.1007/978-981-19-1894-0_10
- [20] R. B. Reckziegel, T. Lowe, T. Devereux, S. M. Johnson, E. Rochelmeyer, L. B. Hutley, T. Doody, and S. R. Levick, "Assessing the reliability of woody vegetation structural characterisation from uav-ls in a tropical savanna," *Science of Remote Sensing*, vol. 11, p. 100178, 2025. DOI: 10.1016/j.srs.2024.100178
- [21] F. Diara and M. Roggero, "Quality assessment of dji zenmuse II and p1 lidar and photogrammetric systems: Metric and statistics analysis with the integration of trimble sx10 data," *Geomatics*, vol. 2, no. 3, pp. 254–281, 2022. DOI: 10.3390/geomatics2030015
- [22] D. Panagiotidis, A. Abdollahnejad, and M. Slavík, "3d point cloud fusion from uav and tls to assess temperate managed forest structures," *International Journal of Applied Earth Observation and Geoinformation*, vol. 112, p. 102917, 2022. DOI: 10.1016/j.jag.2022.102917
- [23] A. Jang, Y. K. Ju, and M. J. Park, "Structural stability evaluation of existing buildings by reverse engineering with 3d laser scanner," *Remote Sensing*, vol. 14, no. 10, p. 2325, 2022. DOI: 10.3390/rs14102325
- [24] M. Salah, M. Farhan, A. Basha, and M. Sherif, "Filtering of 3d point clouds using maximum likelihood algorithm," *Discover Applied Sciences*, vol. 6, no. 8, p. 419, 2024. DOI: 10.1007/s42452-024-05976-1
- [25] S. Y. Teh, H. L. Koh, P. L.-F. Liu, A. I. M. Ismail, and H. L. Lee, "Analytical and numerical simulation of tsunami mitigation by mangroves in penang, malaysia," *Journal of Asian Earth Sciences*, vol. 36, no. 1, pp. 38–46, 2009. DOI: 10.1016/j.jseaes.2008.09.007
- [26] D. Doyen and P. H. Gunawan, "An explicit staggered finite volume scheme for the shallow water equations," in *Finite Volumes for Complex Applications VII-Methods and Theoretical Aspects: FVCA 7, Berlin, June 2014*, Springer, pp. 227–235, 2014. DOI: 10.1007/978-3-319-05684-5_21
- [27] O. Delestre and F. Marche, "A numerical scheme for a viscous shallow water model with friction," *Journal of Scientific Computing*, vol. 48, no. 1, pp. 41–51, 2011. DOI: 10.1007/s10915-010-9393-y
- [28] O. Delestre and U. Razafison, "Numerical scheme for a viscous shallow water system including new friction laws of second order: Validation and application," in *Advances in Hydroinformatics: SIMHYDRO 2014*, Springer, pp. 227–239, 2015. DOI: 10.1007/978-981-287-615-7_16
- [29] G. S. Stelling and S. A. Duinmeijer, "A staggered conservative scheme for every froude number in rapidly varied shallow water flows," *International Journal for Numerical Methods in Fluids*, vol. 43, no. 12, pp. 1329–1354, 2003. DOI: 10.1002/flid.537
- [30] G. Antova and I. Peev, "Comparison on commercial and free software for point cloud processing," *Inżynieria Mineralna*, vol. 1, no. 1, pp. 511–519, 2024. DOI: 10.29227/IM-2024-01-57